

## Catalytic Aerobic Oxidation by a Trianionic Pincer Cr<sup>III</sup>/Cr<sup>V</sup> Couple

Matthew O'Reilly,<sup>†</sup> Joseph M. Falkowski,<sup>†</sup> Vasanth Ramachandran,<sup>§</sup> Mekhala Pati,<sup>§</sup> Khalil A. Abboud,<sup>†</sup> Naresh S. Dalal,<sup>§</sup> Thomas G. Gray,<sup>‡</sup> and Adam S. Veige<sup>\*†</sup>

<sup>†</sup>University of Florida, Department of Chemistry, Center for Catalysis, P.O. Box 117200, Gainesville, Florida 32607,

<sup>‡</sup>Department of Chemistry, Case Western Reserve University, Cleveland, Ohio 44106, and <sup>§</sup>Department of Chemistry and Biochemistry, Florida State University, Tallahassee, Florida 32306

Received October 5, 2009

Aerobic oxidation that incorporates both O atoms into a substrate (PPh<sub>3</sub>) is achieved by employing a Cr<sup>III</sup>/Cr<sup>V</sup>=O catalytic couple. A terphenyl trianionic pincer ligand stabilizes a high oxidation state Cr<sup>V</sup>=O complex, and both the reduced (Cr<sup>III</sup>, IR/X-ray) and oxidized (Cr<sup>V</sup>=O, electron paramagnetic resonance/IR/X-ray) participants in the catalytic cycle are characterized.

Aerobic oxidation of organic substrates, especially catalyzed reactions incorporating both oxygen atoms of O<sub>2</sub>, is advantageous for atom-economy, selectivity, environmental, and monetary considerations.<sup>1</sup> Homogeneous transition metal complexes excel at catalyzing oxo transfers, but relatively few assimilate molecular oxygen.<sup>2,3</sup> The metal complex must

be capable of reducing dioxygen, yet the M–O bond must be weak enough to be spontaneously cleaved by substrate, a particularly difficult recipe to balance.<sup>4</sup>

Considering the propensity of Cr<sup>V</sup> to be reduced to Cr<sup>III</sup> by biological reductants,<sup>5</sup> Cr<sup>V</sup>O is a reasonable fragment as an oxygen-atom-transfer catalyst. An exemplary system is the corrole-ligated<sup>7</sup> Cr<sup>III</sup>/Cr<sup>V</sup>O cycle developed by Gray and co-workers.<sup>3f</sup> During triphenylphosphine (PPh<sub>3</sub>) oxidation, product inhibition and catalyst decomposition limit the turnover number (TON; mol product/mol catalyst) to 33. A perbrominated corrole Br<sub>8</sub>–Cr<sup>V</sup>O delivers its oxygen atom to PPh<sub>3</sub> at a rate of 8200 M<sup>-1</sup> s<sup>-1</sup>, but the reduced Cr<sup>III</sup> reacts slowly with O<sub>2</sub>, epitomizing the delicate balance required. Oxidation of thiophenol to diphenylsulfide is quantitative, but the TON (55) and the turnover frequency (TOF; mol product/mol catalyst·h) were low (~3 h<sup>-1</sup>).

Corroles naturally occupy four equatorial coordination sites. Improved catalytic properties may be envisioned with a catalyst containing more open or labile sites. Trianionic pincer ligands offer the same opportunities to stabilize high oxidation states,<sup>6a</sup> yet only bind three sites.<sup>7</sup> This report details the use of a trianionic OCO<sup>3-</sup> pincer ligand to stabilize Cr<sup>III</sup> and Cr<sup>V</sup> complexes capable of aerobic oxidation of PPh<sub>3</sub>. We mark the first catalytic event for a complex supported by a trianionic pincer ligand. Included within, we characterize both the reduced Cr<sup>III</sup> (IR/X-ray) and the oxidized Cr<sup>V</sup>O (IR/electron paramagnetic resonance (EPR)/X-ray) species in the Cr<sup>III/V</sup> catalytic cycle. Moreover, we conclusively demonstrate that the trianionic pincer ligand enables remarkably swift O<sub>2</sub> activation by creating an open coordination site.

\*To whom correspondence should be addressed. E-mail: veige@chem.ufl.edu.

(1) (a) Funabiki, T. *Oxygenases and Model Systems*; Kluwer: Boston, MA, 1997. (b) Sheldon, R. A.; Kochi, J. K. *Metal-Catalyzed Oxidations of Organic Compounds*; Academic Press: New York, 1981.

(2) (a) Punniyamurthy, T.; Velusamy, S.; Iqbal, J. *Chem. Rev.* **2005**, *105*, 2329–2363. (b) Costas, M.; Mehn, M. P.; Jensen, M. P.; Que, L. *Chem. Rev.* **2004**, *104*, 939–986.

(3) (a) Luobeznova, I.; Raizman, M.; Goldberg, I.; Gross, Z. *Inorg. Chem.* **2006**, *45*, 386–394. (b) Carson, E. C.; Lippard, S. J. *Inorg. Chem.* **2006**, *45*, 837–848. (c) Kim, S. O.; Sastri, C. V.; Seo, M. S.; Kim, J.; Nam, W. J. *Am. Chem. Soc.* **2005**, *127*, 4178–4179. (d) Moreira, R. F.; Tshuva, E. Y.; Lippard, S. J. *Inorg. Chem.* **2004**, *43*, 4427–4434. (e) Carson, E. C.; Lippard, S. J. *J. Am. Chem. Soc.* **2004**, *126*, 3412–3413. (f) Mahammed, A.; Gray, H. B.; Meier-Callahan, A. E.; Gross, Z. *J. Am. Chem. Soc.* **2003**, *125*, 1162–1163. (g) Tshuva, E. Y.; Lee, D.; Bu, W. M.; Lippard, S. J. *J. Am. Chem. Soc.* **2002**, *124*, 2416–2417. (h) Jacobi, B. G.; Laiter, D. S.; Pu, L. H.; Wargocki, M. F.; DiPasquale, A. G.; Fortner, K. C.; Schuck, S. M.; Brown, S. N. *Inorg. Chem.* **2002**, *41*, 4815–4823. (i) Dobler, C.; Mehlretter, G. M.; Sundermeier, U.; Beller, M. *J. Am. Chem. Soc.* **2000**, *122*, 10289–10297. (j) Dobler, C.; Mehlretter, G.; Beller, M. *Angew. Chem., Int. Ed.* **1999**, *38*, 3026–3028. (k) Neumann, R.; Dahan, M. *Nature* **1997**, *388*, 353–355. (l) Groves, J. T.; Quinn, R. J. *Am. Chem. Soc.* **1985**, *107*, 5790–5792. (m) Chin, D. H.; Lamar, G. N.; Balch, A. L. *J. Am. Chem. Soc.* **1980**, *102*, 5945–5947.

(4) (a) Holm, R. H.; Donahue, J. P. *Polyhedron* **1993**, *12*, 571–589. (b) Holm, R. H. *Chem. Rev.* **1987**, *87*, 1401–1449.

(5) (a) Jennette, K. W. *J. Am. Chem. Soc.* **1982**, *104*, 874–875. (b) Connett, P. H.; Wetterhahn, K. E. *J. Am. Chem. Soc.* **1985**, *107*, 4282–4288. (c) Shi, X. L.; Dalal, N. S. *Biochem. Biophys. Res. Commun.* **1988**, *156*, 137–142. (d) Shi, X. L.; Dalal, N. S. *Biochem. Biophys. Res. Commun.* **1989**, *163*, 627–634. (e) Shi, X. L.; Sun, X. Y.; Gannett, P. M.; Dalal, N. S. *Arch. Biochem. Biophys.* **1992**, *293*, 281–286. (f) Ramsey, C. M.; Dalal, N. S. *Mol. Cell. Biochem.* **2004**, *255*, 113–118.

(6) (a) Gross, Z.; Gray, H. B. *Inorg. Chem.* **2006**, *45*, 61–72. (b) Gross, Z.; Gray, H. B. *Adv. Synth. Catal.* **2004**, *346*, 165–170. (c) Meier-Callahan, A. E.; Di Bilio, A. J.; Simkhovich, L.; Mahammed, A.; Goldberg, I.; Gray, H. B.; Gross, Z. *Inorg. Chem.* **2001**, *40*, 6788–6793. (d) Meier-Callahan, A. E.; Gray, H. B.; Gross, Z. *Inorg. Chem.* **2000**, *39*, 3605–3607.

(7) (a) Sarkar, S.; Carlson, A. R.; Veige, M. K.; Falkowski, J. M.; Abboud, K. A.; Veige, A. S. *J. Am. Chem. Soc.* **2008**, *130*, 1116–1117. (b) Sarkar, S.; Abboud, K. A.; Veige, A. S. *J. Am. Chem. Soc.* **2008**, *130*, 16128–16129. (c) Agapie, T.; Day, M. W.; Bercaw, J. E. *Organometallics* **2008**, *27*, 6123–6142. (d) Koller, J.; Sarkar, S.; Abboud, K. A.; Veige, A. S. *Organometallics* **2007**, *26*, 5438–5441. (e) Agapie, T.; Bercaw, J. E. *Organometallics* **2007**, *26*, 2957–2959.

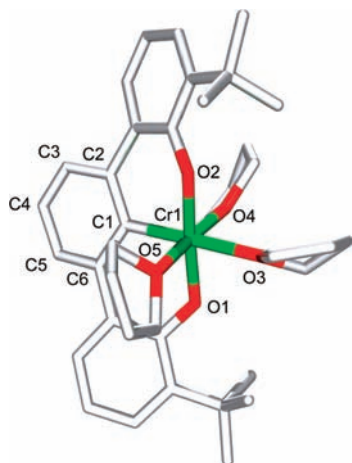
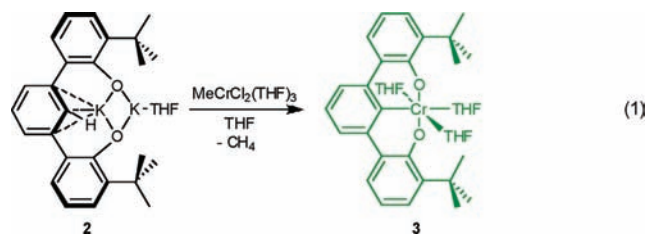


**Figure 1.** Molecular structure of  $[\text{t-BuOCO}]\text{Cr}^{\text{III}}(\text{THF})_3$  (**3**).

We sought a mild metalation strategy that combines double salt metathesis with C–H bond activation. Thus, we synthesized the dipotassium derivative  $(\text{t-BuOCO})\text{HK}_2(\text{THF})$  (**2**) by treating  $(\text{t-BuOCO})\text{H}_3$  (**1**) with potassium hydride (KH) in THF (see the Supporting Information for X-ray details). Upon the addition of **2** to  $\text{MeCrCl}_2(\text{THF})_3$  in THF, the solution instantly darkens from lime green to dark green (eq 11). After 5 h, solvent removal provides a green solid. This is extracted into toluene, and KCl is removed by filtration. After removing the toluene in vacuo, the solids remaining are dissolved in minimal THF and cooled to  $-35^\circ\text{C}$  to induce crystallization and produce analytically pure **3** in 44% yield.



A  $^1\text{H}$  NMR spectrum of **3** reveals paramagnetically shifted and broadened resonances. The signals appear at 8.20 ( $\nu_{1/2} = 518$ ), 1.45 ( $\nu_{1/2} = 1035$ ; t-Bu),  $-7.44$  ( $\nu_{1/2} = 645$ ),  $-13.23$  ( $\nu_{1/2} = 750$ ), and  $-22.71$  ( $\nu_{1/2} = 2520$ ) ppm. No resonances are observed in the  $^{13}\text{C}\{^1\text{H}\}$  NMR spectrum of **3**. Although the  $^1\text{H}$  NMR spectrum is not useful for confirming the identity of **3**, there is enough information available (location of resonances and  $\nu_{1/2}$ ) to determine if subsequent reactions lead to new chromium-containing products.

Single crystals grow by cooling a concentrated solution of **3** in THF to  $-35^\circ\text{C}$ . Exemplifying the reactivity of **3** toward  $\text{O}_2$ , crystals of **3** immersed in Paratone 8277 oil (Exxon) darken within minutes and must be cooled with dry ice prior to crystal selection for X-ray analysis. Figure 1 depicts the molecular structure of **3**, which consists of a distorted octahedral  $\text{Cr}^{\text{III}}$  ion coordinated by the  $\text{OCO}^{3-}$  pincer and three THF ligands. The mutually *trans*-THF ligands and two lattice THF molecules (not shown) are disordered. The OCO pincer ligand adopts a pseudo  $C_2$ -symmetric orientation. A strong *trans* influence from the Cr–C1 bond ( $d(\text{Cr1}–\text{C1}) = 2.011(3)$  Å) causes a 0.14 Å elongation in the Cr1–O3 bond length ( $d(\text{Cr1}–\text{O3}) = 2.1939(18)$  Å) compared to Cr1–O4 ( $d(\text{Cr1}–\text{O4}) = 2.0624(18)$  Å) and Cr1–O5

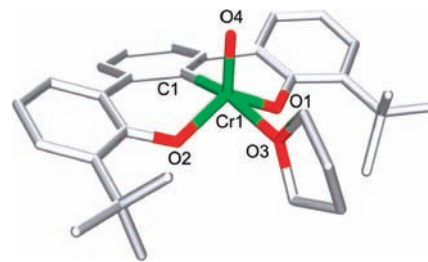
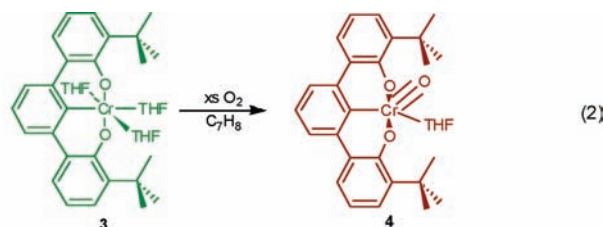


**Figure 2.** Molecular structure of  $[\text{t-BuOCO}]\text{Cr}^{\text{V}}=\text{O}(\text{THF})$  (**4**).

( $d(\text{Cr1}–\text{O5}) = 2.0566(18)$  Å). As expected, shorter bonds form between the  $\text{Cr}^{\text{III}}$  ion and the alkoxide attachments ( $d(\text{Cr1}–\text{O1}) = 1.9227(17)$  Å and  $d(\text{Cr1}–\text{O2}) = 1.9248(17)$  Å).

When treating **3** with an excess of  $\text{O}_2$  (1 atm) in toluene, the  $\text{Cr}^{\text{V}}\text{O}$  complex  $[\text{t-BuOCO}]\text{Cr}^{\text{V}}=\text{O}(\text{THF})$  (**4**) forms immediately (eq 22), and the solution color changes from bright green to red-brown. The  $^1\text{H}$  NMR spectrum of **4** exhibits several broad paramagnetically shifted resonances at 11.4, 9.0, 4.3, 2.4, and 1.2 ppm. The addition of THF to the NMR tube causes the signal at 1.2 ppm to grow and is attributable to a bound THF capable of rapid exchange with free THF. In the solid state, **4** is brown, and the  $\text{Cr}^{\text{V}}=\text{O}$  stretch appears as a strong absorption at  $988\text{ cm}^{-1}$  and shifts to  $943\text{ cm}^{-1}$  for the  $\text{Cr}^{\text{V}}=^{18}\text{O}$  derivative.<sup>8</sup>



An EPR spectrum (see the Supporting Information) of a 10 mmol solution of **4** in toluene exhibits a strong resonance at  $g_{\text{iso}} = 1.9770$ . The central line corresponds to the allowed ( $\Delta M_S = \pm 1$ ) electron spin transition from the ( $S = 1/2$ ,  $I = 0$ )  $^{52}\text{Cr}$  isotope. The four weak satellites represent the  $^{53}\text{Cr}$  ( $I = 3/2$ ) hyperfine structure, yielding a hyperfine constant of 19 G (1.9 mT), consistent with a  $\text{Cr}^{\text{V}}$  ion.<sup>9</sup> The UV–vis spectrum of **4** reveals ligand-to-metal charge transfer absorptions in the UV region at 250 nm and at 285 nm and a weak d–d transition at 500 nm.

Figure 2 shows the molecular structure of the  $\text{Cr}^{\text{V}}=\text{O}$  complex **4** obtained by single-crystal X-ray analysis and confirms the presence of an oxo ligand. Complex **4** consists of a  $\text{Cr}^{\text{V}}$  ion in a distorted trigonal bipyramidal (tbp) geometry that consists of the OCO trianionic pincer, the oxo, and a THF molecule in one of the axial positions. The oxo ligand occupies an equatorial position with a typical Cr–O bond length of 1.5683(18) Å.<sup>8</sup> The  $\angle\text{C1}–\text{Cr}–\text{O3}$  angle of  $165.27(8)^\circ$  is significantly distorted from linearity,

(8) For some structurally characterized  $\text{Cr}^{\text{V}}-\text{oxo}$  complexes, see ref 7d, (a) Collins, T. J.; Slobodnick, C.; Uffelman, E. S. *Inorg. Chem.* **1990**, *29*, 3433–3436 and ref 6 therein, and (b) Egorova, O. A.; Tsay, O. G.; Khatua, S.; Huh, J. O.; Churchill, D. G. *Inorg. Chem.* **2009**, *48*, 4634–4636. (c) Odum, A. L.; Mindiola, D. J.; Cummins, C. C. *Inorg. Chem.* **1999**, *38*, 3290–3295. (d) Noh, S. K.; Heintz, R. A.; Haggerty, B. S.; Rheingold, A. L.; Theopold, K. H. *J. Am. Chem. Soc.* **1992**, *114*, 1892–1893. (e) Morse, D. B.; Rauchfuss, T. B.; Wilson, S. R. *J. Am. Chem. Soc.* **1988**, *110*, 8234–8235.

(9) Dalal, N. S.; Millar, J. M.; Jagadeesh, M. S.; Seehra, M. S. *J. Chem. Phys.* **1981**, *74*, 1916–1923.

caused in part by the strain of the terphenyl ligand and the short Cr=O bond. The equatorial atoms create angles of 116.73(9)°, 115.82(9)°, and 126.89(8)°, signifying a coordination geometry closer to *tbp* than to square pyramidal. This is the first example of a *tbp* Cr(V)–oxo complex.<sup>8</sup>

Spin-unrestricted density-functional theory calculations<sup>10</sup> were performed on **4'**, an analogue of **4** having methyl groups in place of *t*-butyl. Computational details appear in the Supporting Information. Full geometry optimization converged on a potential-energy minimum, as confirmed by a harmonic vibrational frequency calculation. The optimized structure captures the trigonal bipyramidal geometry about chromium. The computed bond distances agree well with crystallographic values: the calculated (experimental) chromium–oxo oxygen bond length is 1.569 Å (1.5683(18) Å); the Cr–O<sub>pincer</sub> distances are 1.819 Å (1.8166(17) Å) and 1.815 Å (1.8098(17) Å), and that to the THF oxygen atom is 2.243 Å (2.1781(17) Å). The calculated Cr–C<sub>pincer</sub> bond length is 1.992 Å (2.009(2) Å, experimental). The calculated *g* factor agrees well with the experimental data (1.9970<sub>exptl</sub>/1.969<sub>calcd</sub>). The short distance between chromium and the oxo ligand suggests multiple-bond character, and the Wiberg bond order is 2.15.<sup>11</sup> Corresponding Cr–O bond orders to the pincer ligand oxygen atoms are 1.00 and 1.04. The THF ligand is weakly held, with a Cr–O bond order of 0.27.

The unpaired electron (*S* = 1/2) resides in an orbital of mixed Cr–pincer ligand parentage. The highest occupied and lowest unoccupied Kohn–Sham orbitals are majority-spin ( $\alpha$ ) functions. A Mulliken population analysis<sup>12</sup> assigns 21% of the  $\alpha$ -HOMO (HOMO = highest occupied molecular orbital) density to Cr and 79% to the anionic pincer. The  $\alpha$ -LUMO (LUMO = lowest unoccupied molecular orbital) is primarily a Cr–O  $\pi^*$  combination, with 62% Cr, 26% oxo, 2.6% pincer ligand, and 9.4% THF character. The Cr–O  $\pi^*$  orbital is a reasonable point of attack by external nucleophiles such as PPh<sub>3</sub>.

Indeed, in the presence of 1 atm of O<sub>2</sub>, the reduced Cr<sup>III</sup> complex **3** catalytically oxidizes PPh<sub>3</sub> to O=PPh<sub>3</sub> with a TON of 195. The catalysis works on a bulk scale. Within 3 h, 0.68 g of O=PPh<sub>3</sub> (2.44 mmol) forms with only 8 mg (0.0125 mmol) of the catalyst. In an NMR tube reaction, consumption of 10 equiv of PPh<sub>3</sub> occurs before obtaining the first spectrum (~5 min), which correlates to a minimum turnover frequency of 100 h<sup>-1</sup>. In the presence of excess O<sub>2</sub>, after consumption of all of the PPh<sub>3</sub>, the red-brown color of the Cr<sup>V</sup>O persists, but upon reintroduction of more substrate, the catalysis resumes. Catalytic turnover with **4** also occurs when air is the source of O<sub>2</sub>. Complex **4** is unable to oxidize styrene, dimethylsulfide, dimethylsulfoxide, or triethylamine.

The reaction of O<sub>2</sub> with **3** is fast; no isolable or detectable intermediate appears in sufficient quantity. In the absence of PPh<sub>3</sub>, a Cr<sup>IV</sup>–O–O–Cr<sup>IV</sup> intermediate may precede O–O bond cleavage to provide 2 equiv of Cr<sup>V</sup>=O. To confirm this dioxygenase model, treating **3** with a stoichiometric amount of <sup>18</sup>O<sub>2</sub> and PPh<sub>3</sub> provides >98% <sup>18</sup>O=PPh<sub>3</sub> quantitatively.

During the catalytic reaction, a broad resonance appears in the <sup>31</sup>P{<sup>1</sup>H} NMR spectrum at 26.18 ppm, and as more product builds, the resonance migrates to the position of free O=PPh<sub>3</sub> at 30.11 ppm. This is attributable to a phosphine–

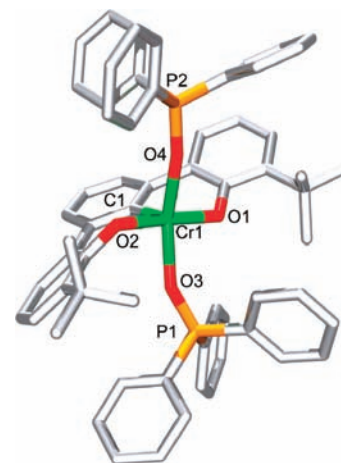


**Figure 3.** Molecular structure of [*t*-BuOCO]Cr<sup>III</sup>(OPPh<sub>3</sub>)<sub>2</sub> (**5**).

oxide bound Cr<sup>III</sup> complex in exchange with free O=PPh<sub>3</sub>. Variable-temperature experiments did not resolve the dynamic interaction, indicating a rapid exchange. An authentic sample of the bisphospine Cr<sup>III</sup> complex [*t*-BuOCO]Cr<sup>III</sup>–(OPPh<sub>3</sub>)<sub>2</sub> (**5**) forms upon treating [*t*-BuOCO]Cr<sup>III</sup>(THF)<sub>3</sub> (**3**) with 2 equiv of O=PPh<sub>3</sub>. The <sup>31</sup>P{<sup>1</sup>H} NMR spectrum of **5** does not exhibit a signal due to the paramagnetic d<sup>3</sup> Cr<sup>III</sup> ion, but when 5 equiv of O=PPh<sub>3</sub> are added to the sample, the same signal appears at 26.18 ppm. Notably, **5** will also catalyze the oxidation of PPh<sub>3</sub> within 1 atm of O<sub>2</sub> and air. Single crystals form in supersaturated CH<sub>2</sub>Cl<sub>2</sub> solutions, and an X-ray analysis provides the molecular structure (Figure 3).

Complex [*t*-BuOCO]Cr<sup>III</sup>(OPPh<sub>3</sub>)<sub>2</sub> (**5**) is square-pyramidal with C<sub>2v</sub> symmetry in which the pincer-carbon atom is apical and the two Cr–O alkoxides and O=PPh<sub>3</sub> fulfill the basal positions. The pyramidal base is distorted along the *trans*-O=PPh<sub>3</sub> ligands (∠O3–Cr–O4 = 157.38(5)°) but nearly linear across the *trans*-alkoxides (∠O1–Cr–O2 = 175.28(5)°). The defining feature of **5** is the open coordination site opposite the Cr–C1 bond. Consequently, of the three compounds within this study, **5** presents the shortest Cr–C<sub>pincer</sub> bond of 1.9761(17) Å. Complex **5** provides an accessible binding site for O<sub>2</sub> to facilitate activation that offers a plausible explanation for the rapid oxidation.

In summary, a trianionic pincer ligand is capable of stabilizing a high oxidation state Cr<sup>V</sup>=O, d<sup>1</sup> complex that participates in catalytic aerobic oxidation of PPh<sub>3</sub>. The TON (195), relative to the corrole system (**33**), suggests that the additional labile/open coordination site is advantageous, and a broad scope of catalysis featuring tetradentate ligands may be significantly improved by switching to a trianionic pincer ligand.

**Acknowledgment.** A.S.V. thanks UF, the ACS–PRF(G) (#44063-G3), NSF CAREER (CHE-0748408), and the Camille and Henry Dreyfus Foundation T.G.G. thanks the NSF (CHE-0749086) and the Alfred P. Sloan Foundation.

**Note Added after ASAP Publication.** This paper was released ASAP on November 6, 2009. An additional minor text correction was made and the correct version posted on November 10, 2009.

(10) Martin, C. H.; Zerner, M. C. In *Inorganic Electronic Structure and Spectroscopy*; Solomon, E. I.; Lever, A. B. P., Eds.; Wiley: New York, 1999; Vol. I, 555–660.

(11) Wiberg, K. B. *Tetrahedron* **1968**, *24*, 1083–1096.

(12) Mulliken, R. S. *J. Chem. Phys.* **1955**, *23*, 1833–1840.

**Supporting Information Available:** Full experimental procedures, NMR spectra, IR, and X-ray crystallographic details. This material is available free of charge via the Internet at <http://pubs.acs.org>.